NIH-PA Author Manuscript

NIH-PA Author Manuscript

NIH-PA Author Manuscript

Generation of Cancerous Neural Stem Cells Forming Glial Tumor by Oncogenic Stimulation

Ji-Seon Lee,
Department of Life Sciences, Sogang University, Seoul 121–742, Korea

Hong Jun Lee,
Medical Research Institute, Chung-Ang University College of Medicine, Seoul, Korea. Division of Neurology, Department of Medicine, UBC Hospital, University of British Columbia, Vancouver, BC V6T 2B5, Canada

Bo-Hyun Moon,
Department of Biochemistry and Molecular & Cellular Biology, Georgetown University, Washington, DC, USA

Seung-Hyun Song,
Department of Biomedical Sciences, CHA University, Seoul, Korea

Mi-Ok Lee,
Department of Biomedical Sciences, CHA University, Seoul, Korea

Sung Han Shim,
Department of Biomedical Sciences, CHA University, Seoul, Korea

Hyung Seok Kim,
Department of Forensic Medicine, Chonnam National University Medical School, Gwangju, Korea

Min Cheol Lee,
Department of Pathology, Chonnam National University Medical School, Gwangju, Korea

Jeong Taik Kwon,
Department of Neurosurgery, Chung-Ang University College of Medicine, Seoul, Korea

Albert J. Fornace Jr.,
Department of Biochemistry and Molecular & Cellular Biology, Georgetown University, Washington, DC, USA

Seung U. Kim, and

Correspondence to: Hyuk Jin Cha, hjcha@sogang.ac.kr.

Ji-Seon Lee and Hong Jun Lee contributed equally to this work.

Medical Research Institute, Chung-Ang University College of Medicine, Seoul, Korea. Division of Neurology, Department of Medicine, UBC Hospital, University of British Columbia, Vancouver, BC V6T 2B5, Canada

Hyuk Jin Cha
Department of Life Sciences, Sogang University, Seoul 121–742, Korea

Hyung Seok Kim: sukim@interchange.ubc.ca; Hyuk Jin Cha: hjcha@sogang.ac.kr

Abstract

Neural stem cells in the brain have been shown to be 'cells of origin' of certain brain cancers, most notably astrocytomas and medulloblastoma. In particular, in a mouse model, the targeting of genetic modifications for astrocytoma-relevant tumor suppressors to neural stem cells causes malignant astrocytoma to arise, thereby suggesting that astrocytoma is derived from neural stem cells. However, it remains to be determined whether this important finding is reproducible in humans. Herein, we generated cancerous neural stem cells by introducing a set of oncogenes to human fetal neural stem cells (hfNSCs). Serial genetic modification with v-myc for immortalization and consequent H-Ras for oncogenic stimulation with viral gene delivery proved sufficient to induce the transformation of hfNSCs. The resultant F3.Ras cells evidenced a variety of the hallmarks of brain cancer stem cells and most importantly were tumorigenic, forming brain cancers consisting of both a large number of differentiated and a very few undifferentiated populations of cells in an in vivo mouse model. On the contrary, oligodendrocytes derived from the v-myc expressing parent neural stem cells were not transformed by H-Ras, which suggests that neural stem cells may be more susceptible to cancerous transformation by a combination of oncogenes. We also determined that v-myc expressing fetal neural stem cells were defective in p53 response upon the introduction of H-Ras; this finding suggests that an insufficient p53-dependent tumor suppressive mechanism would be associated with high oncogenic susceptibility to H-Ras introduction.

Keywords

Human neural stem cells; v-myc; H-Ras; Cancerous stem cells; p53; Glial tumor

Introduction

The neoplastic transformation of fully differentiated glia has been previously implicated as the principal cause of gliomagenesis [1]. This idea is supported by the findings of prior studies reporting that glioma formation from normal human astrocytes could be achieved via the ectopic expression of a number of oncogenes—SV40 *T/t-Ag*, H-*ras,* and *hTERT* [2]. Because adult glial cells are generally believed to be the only cells that divide in the postnatal brain, they may represent a vulnerable target for neoplastic transformation by a variety of oncogenic mutations, including *p53, PTEN, NF1, EGFR, ERBB2,* and *RB1,* which are frequently shown to be mutated in brain cancers, as previously demonstrated in mouse model studies [3, 4]. However, the results of recent studies have shown that neural stem cells and glial progenitor cells, both of which retain their proliferative capacity, were detected in multiple regions of the postnatal brain [1, 5, 6]. Therefore, classic theories

regarding the cells of origin of brain cancers must be reconsidered. In this regard, some brain cancers—particularly glioblastoma and medulloblastoma, which frequently occur in cases of pediatric brain cancer—have reportedly been derived from neural stem cells [7, 8]. The inactivation of several tumor suppressors, including *p53, NF1,* and *PTEN* in neural stem/precursor cells located within the subventricular zone (SVZ), results in the formation of malignant astrocytoma [9]. The results of several previous studies have shown that neural stem/progenitor cells may prove more susceptible to malignant transformation [7, 9].

Interestingly, human somatic cells, including astrocytes, have generally been considered to be more resistant to oncogenic transformation than murine somatic cells, owing to their intrinsic tumor suppressive mechanisms [10]. Human somatic cells require at least three genetic events for cellular transformation: immortalization, self-sufficient growth control, and the abrogation of the tumor-suppressive mechanism [11]. The tumor-suppressive mechanism, which is frequently governed by the p53 tumor suppressor, carries out a pivotal function in preventing the transformation of normal cells. In the majority of human gliomas, the disruption of the tumor-suppressive mechanism (the p53 and Rb pathway) in parallel with abnormally active signals (Ras and telomerase) has been demonstrated [12]. It has also been shown that a simultaneous alteration satisfying three genetic events (immortalization, self-sufficient growth control, and abrogation of the tumor-suppressive mechanism) is required for the transformation of human astrocytes [2]. Therefore, the abrogation of the p53-dependent tumor suppressive mechanism is indispensible in the transformation occurring in response to a variety of oncogenic stimuli [13–15].

In this study, we demonstrate that the serial introduction of v-myc and H-Ras was sufficient for the transformation of hfNSCs, which evidenced some characteristics of cancer stem cells. F3.Ras cells induced the formation of peripheral neuroepithelioma (PNET)-like cancer masses in nude mouse brains. Furthermore, the molecular mechanism involved in hfNSCs transformation was linked to defective p53 responses in v-myc expressing hfNSCs.

Materials and Methods

Generation of v-myc Expressing Human Fetal Neural Stem Cells

The amphotropic replication-incompetent retroviral vector pLSN.v-*myc* was used to infect human brain cells isolated from fetal brains at 15 weeks of gestation. Permission to use the fetal tissues was granted by the Clinical Research Screening Committee involving Human Subjects of the University of British Columbia. The pLSN.v-myc vector was generated using the ecotropic retroviral vector encoding for v-myc, in a fashion similar to that described previously for the generation of hfNSC lines [16–18]. The PA317 amphotropic packaging cell line was infected with the pLSN.v-myc vector, and successful infectants were selected and expanded. Supernatants generated from the PA317 producer cell line (PASK1.2) harbored replication-incompetent retroviral particles bearing an amphotropic envelope which efficiently infected the hfNSCs, as indicated by the observed G-418 resistance. Two milliliters of culture supernatant from the packaging cell line and 8 μg/ml of polybrene were added to the brain cells in six-well plates and incubated for 24 h at 37°C. The medium was subsequently replaced with fresh growth medium; the infection procedure was repeated 24 and 48 h later. 72 h after the third infection procedure, the infected cells

were selected for 14 days with G-418 (200 μg/ml), and large clusters of cells were individually isolated and grown in dishes coated with poly-L-lysine. Individual clones (*n*=3) were again selected via limited dilution and further propagated. The resultant v-myc-expressing hfNSCs were referred to as HB1.F3 and were used in the present study. F3 NSCs were cultivated in a serum-free medium (DM4) consisting of DMEM with high glucose containing 10 μg/ml insulin, 10 μg/ml transferrin, 30 nM sodium selenate, 50 nM hydrocortisone, and 0.3 nM T3. the DM4 was supplemented with recombinant human basic fibroblast growth factor (bFGF, 10 ng/ml; PeproTech, Rocky Hill, NJ) during routine feeding. All chemicals except bFGF were purchased from Sigma-Aldrich (St. Louis, MO). F3 NSCs were also maintained in DMEM medium supplemented with 10% (v/v) fetal bovine serum (FBS) with 20 μg/mL of gentamycin (Sigma) at 37°C in a humidified 5% CO_2 incubator.

Generation of Cancerous Neural Stem Cells by Introducing H-Ras

HB1.F3 (F3) cells were further transduced with pBabe-H-Ras^{G12V} retroviral vector to generate the new human neural stem cell line HB1.F3.Ras (F3.Ras) encoding for both v-*myc* and Ras. In brief, each viral plasmid (20 μg, pBabe (Cont), and pBabe-H-Ras^{G12V}) was transfected into Phoenix Amphor viral packaging cells (5×10^6) using Lipofectamine 2000 (Invitrogen, #11668-027). After 48 h, culture media containing the viruses were collected from the transfected Phoenix cells and subsequently filtered (0.45 μm filter, Millipore). Target F3 cells plated at a density of 8×10^5 were incubated with the virus-containing medium for 48 h, in the presence of 4 μg/ml of polybrene (Sigma). The infection procedure was repeated 24 and 48 h later. 72 h after the third infection procedure, infected cell populations were selected via the addition of 0.5 μg/ml of puromycin to the medium. Three large colonies of cells were individually isolated and grown via limited dilution and further propagated.

Reagents

Primary antibodies against Nestin (10c2: sc-23927), H-Ras (c-20: sc520), cyclin B1 (GNS1: sc-245), cyclin E (sc-198), ki-67 (H-300: sc-15402), β-actin (sc-47778), and GFAP (sc-9973) were obtained from Santa Cruz Biotechnology. Primary antibodies against phosphorylated Rb (pRb, ser795: # 9301), phosphorylated Akt (pAkt, ser473: # 4060X), phospho-Histone H3 (Ser10: # 9706), phosphorylated p42/44 (ppERK, # 9106), and E-cadherin (# 4065) were acquired from Cell Signaling Technology (Danver, MA). Primary antibodies against Snail (# ab17732), and Sox2 (# ab15830) were acquired from Abcam (Cambridge, MA). Secondary antibody Alexa 594-conjugated goat anti-mouse IgG was purchased from Molecular Probes (Eugene, OR), and Cy2-conjugated goat anti-rabbit IgG from Jackson ImmunoResearch (Wes Grove, PA).

Generation of Tumorspheres

Tumorspheres were generated by culturing F3 and F3.Ras cells in DMEM/F12 supplemented with 2% B27, 8 mM HEPES, 100 U/mL of penicillin, 100 μg/mL of streptomycin and 20 ng/mL of bFGF (invitrogen, Carlsbad, CA) for 7 days.

Immunoblotting

The cells were washed twice in ice-cold phosphate buffered saline (PBS), lysed with 300 μl of tissue lysis buffer, and centrifuged for 10 min at 14,000 rpm (to clarify the lysates). Approximately 20 μg of total proteins were separated via SDS-PAGE. The proteins were then transferred to PVDF membranes, blocked for 1 h with 5% nonfat dry milk in Tris-buffered saline (TBS) with 0.1% Tween-20 (TBS-T), and incubated for 1 to 16 h with the appropriate primary antibodies in TBS containing 1% BSA solution. The membranes were subsequently washed several times in TBS-T solution and incubated with HRP-conjugated secondary antibodies (0.1 μg/ml; Jackson ImmunoResearch Laboratories, West Grove, PA). Immunoreactivity was detected using an enhanced chemiluminescence detection system (Amersham Biosciences, Piscataway, NJ).

Immunofluorescence

Cells cultivated on round glass coverslips were fixed with 4% paraformaldehyde in 0.1 M phosphate buffer (pH 7.2) for 10 min, and subsequently permeabilized for 5 min with 0.1% Triton X-100 in PBS. The fixed cells were incubated in TBS containing 3% BSA (for blocking) for 30 min, followed by 1 h of incubation with specific primary antibodies. The cells were washed 3 times in TBS-T solution, then incubated with Alexa 594-conjugated goat anti-mouse or Cy2-conjugated goat anti-rabbit IgGs. Cellular nuclei were counterstained with 4′,6-diamidino-2-phenylindole (DAPI, 0.2 μg/mL) in PBS.

Immunohistochemistry

The tumor tissues from mice injected dermally with F3.Ras and U373 human glioma cells were fixed in phosphate-buffered 10% formalin and the tissue samples were embedded in paraffin. The paraffin sections were deparaffinized, rehydrated, and subjected to citrate-based antigen retrieval. Primary antibodies specific for GFAP, Nestin, ki-67, and phospho-Histone H3 were used. The secondary antibodies used were Alexa 594-conjugated goat anti-mouse or Cy2-conjugated goat anti-rabbit IgGs for immunofluorescence, and ABC kits (Vector Laboratory) for HRP staining. The sections were also stained with hematoxylin and eosin (H&E) for histopathological analysis.

RNA Isolation and Quantitative Real-Time PCR Analysis

Total RNA was extracted from the cells using TRIzol Reagent (Invitrogen), followed by treatment with DNase I, in accordance with the manufacturer's instruction. Trizol was removed via the addition of chloroform, and mRNA was precipitated with isopropanol. The RNA precipitates were washed with 75% ethanol. The quantity and purity of RNA were assessed by optical density measurements at 260 nm and 280 nm using an UV spectrometer, and the integrity of the RNA was confirmed via agarose gel electrophoresis. Gene-specific primers were designed to amplify human Sox2 (forward: 5′-ATGCACCGCTACGACGTGA-3′, reverse: 5′-CTTTTGCACCCCTCCCATTT-3′); hNestin (forward: 5′-AGAAGAGGACCAGAGTATTGT GAG-3′, reverse: 5′-TCCGTCGCTGTTGAG TCTC-3′); human ABCG2 (forward: 5′-TTAAGTGGAAACTGCT GCTTT AGGT-3′, reverse: 5′-TCGGTCTTAACCAAAGGCTCA-3′) and the housekeeping gene GAPDH. All

amplifications were conducted in a pre-mixture (20 μl) containing 500 nmol/l of gene-specific primers, and 2 ml of template, under the following conditions: denaturation at 95°C for 1 min, followed by 30 cycles of 95°C for 30 s, 58°C for 30 s, and 72°C for 30 s, with a final extension at 72°C for 5 min. For PCR validation, amplified products were separated on 2% agarose gels and visualized by ethidium bromide staining. p53 dependent gene expression was demonstrated by RT^2 profiler PCR array human p53 Signaling Pathway as described by the manufacturer. The reactions were carried out in an Applied Biosystems 7500 Fast-Real Time PCR System (Applied Biosystems, Foster City, CA).

Soft Agar Assay

Each well of a 6-well plate was coated with 3 ml of bottom agar mixture (DMEM, 10% FBS, and 0.6% agar). After the bottom layer solidified, 2 ml of top agar mixture (DMEM, 10% FBS, and 0.3% agar) containing 5×10^5 cells was added to each well, and the cultures were incubated at 37°C in a 5% CO_2 atmosphere. Every 5 days, normal growth medium was layered gently over the cultures. Colony formation was monitored daily using a light microscope. Colonies formed in soft agar were photographed with a digital camera after 14 days of incubation.

Fluorescent In Situ Hybridization (FISH)

FISH was conducted using two human chromosome-specific probes, LSI 21 (Spectrum Orange, Abbott Laboratories, Chicago, IL) and CEP18 (Spectrum Green, Abbott). Slides and probe preparation were carried out in accordance with the routine FISH protocol. Probe hybridization was conducted using a Hybrite system (Abbott) at 37°C for 16 h. After post-hybridization washing, the slide was counterstained with 4′6′-diamino-2-phenylindole dihydrochloride (DAPI). The FISH signals were captured with a Cytovision system v3.6 (Applied Imaging, London, UK).

Transplantation of Transformed Cells in Mouse Muscle and Brain

NOD/SCID male mice at 6 weeks of age were subcutaneously injected with 1×10^6 F3.pBabe or F3.Ras cells in the thigh muscle, and tumor appearance after 6 weeks was monitored. Tumor masses from the right thigh area injected with F3.Ras cells were isolated and processed for histology. The isolated tumor masses were fixed in 4% paraformaldehyde in 0.1 M phosphate buffer (pH 7.4), processed into paraffin sections, and stained with hematoxylin and eosin (H/E). The tumor tissue sections were immunostained with proliferation markers (phospho-Histone H3) and cell type-specific markers for astrocytes (GFAP), proliferation markers (Ki-67) and cell type-specific markers for neural stem cells (hNestin). In like manner, F3 and F3.Ras cells were injected intracerebrally into NOD/SCID mice. Paraffin sections prepared from the brains of the mice were processed for H/E, phospho-Histone H3, hNestin, GFAP, and Ki-67 staining.

Results

Generation of Human Neural Stem Cells Encoding v-myc and Ras

The stable expression of v-myc in hfNSCs exerted no distinct effect on cellular morphology or chromosome karyotyping compared to the parent hfNSCs (Fig. 1a, upper panels and

Supplemental Figure. 1). Even after v-myc expression, levels of human Nestin (hNestin) or Sox2 expression were comparable to the parent hfNSCs, but not in the human dermal fibroblasts (hDFs) (Fig. 1a, bottom panels and right panels). Thereafter, v-myc-expressing hfNSCs (F3) cells were used for further genetic modification. The constitutively active form of H-Ras was expressed stably in F3 cells, generating F3.Ras cells. Unlike the F3 cells, which maintained the morphology of the parent hfNSCs, the F3.Ras cells were clearly morphologically altered (Fig. 1b). The morphology of the F3.Ras cells was similar to the typical morphology of transformed cells (e.g. condensed cytoplasm, focus formation, and loss of contact inhibition) as reported elsewhere [19]. In order to validate the effects of H-Ras, the characteristic signals of H-Ras activation, including ERK and Akt activation, were evaluated via immunoblotting. As anticipated, both phosphorylated ERK and Akt were highly and constitutively activated in F3.Ras cells with stable H-Ras expression (Fig. 1c). It has been relatively well established that ERK and Akt activations induced by mitogenic or oncogenic signals are responsible for accelerated proliferation compared to both F3 and F3.pBabe cells (left panel Fig. 1d). The proliferation of F3.Ras cells is correlated with the upregulation of a variety of cell cycle regulators, including cyclin B1 and cyclin E, and subsequent Rb hyperphosphorylation (right panel, Fig. 1d). As an assay of cellular transformation, anchorage-independent growth was measured by the growth rate assessed on soft-agar. As compared to the E1a/Ras mouse embryonic fibroblast (MEF) used as a positive control, the numbers of F3.Ras colonies grown on soft-agar were comparable to those of E1a/Ras MEF, thereby indicating that the F3.Ras cells were indeed transformed (Fig. 1e).

F3.Ras Cells Retain Cell Type-Specific Markers for Neural Stem Cells

F3 cells express characteristic phenotypes of hfNSCs, and also express characteristics NSC markers such as hNestin (Fig. 1a, right panel) and the ATP-binding cassette transporter (ABCG2) [20]. We therefore attempted to determine whether the introduction of H-Ras to the F3 cells altered the neural stemness of the F3 cells. In order to answer this question, we determined the levels of hNestin and SRY box-containing gene 2 (Sox2), both of which are utilized extensively for the identification of neural stem/progenitor cells [21]. As shown in Fig. 2a, both hNestin and Sox2 were clearly stained in both F3 and F3.Ras cells, but not in human bone marrow mesenchymal stem cells (hMSCs) (Fig. 2a). Similarly, the mRNA of Sox2 and hNestin were expressed in both F3 and F3.Ras cells (Fig. 2b). Interestingly, the levels of Sox2 and hNestin protein in F3.Ras cells appeared to have moderately increased relative to what was observed in the F3 cells (Fig. 2c). Therefore, the F3.Ras cells apparently retain neural stemness characteristics similar to those of F3 cells, even after cellular transformation. Under sphere culture conditions, F3.Ras cells formed larger-sized spheres than the control F3 cells (Fig. 2d).

F3.Ras Cells Share Characteristics of Cancer Stem Cells

We subsequently attempted to determine whether or not the F3.Ras cells share any properties in common with neural cancer stem cells isolated from adult or pediatric brain cancers, as has been reported in a number of previous studies [22–24]. In this comparison, we initially compared the levels of ABCG2, one of the ABC transporters, which is expressed abundantly in brain tumor stem cells [25, 26]. The levels of ABCG2 mRNA were markedly upregulated in F3.Ras cells (Fig. 3a). Recently, aldehyde dehydrogenease 1

(ALDH1) was implicated as a novel cancer stem cell marker that might prove useful in the identification of a variety of stem-like cancer cells from the breast [27], lung [28], colorectal region [29], and head and neck [30] cancers, as well as circulating tumor cells [31]. As anticipated, the levels of ALDH1 mRNA were induced significantly in F3.Ras (Fig. 3b). Next, the levels of E-cadherin protein were determined in order to evaluate the epithelial mesenchymal transition (EMT), which has been identified as either the cause or consequence of cancer stem cells [32–35]. As is shown in Fig. 3c, the F3.Ras cells evidenced a marked loss of E-cadherin relative to the F3 cells, which indicates that the F3.Ras cells had undergone EMT. Interestingly, Snail, which is known to be responsible for the suppression of E-cadherin expression, was upregulated to a significant degree in F3.Ras cells (Fig. 3c middle panel). In sequence, F3 and F3.Ras cells is comparable to fetal NSC, U87 glioma cell line, and U87 sphere stem-like cancer cells. As predicted, c-myc expression was found in both F3 and F3.Ras cells since F3 cells were generated by introducing v-myc to the fetal neural stem cells (fNSCs). Strong H-Ras expression was found in only in F3. Ras cells. Consistently, strong phospho-Rb level was distinct in F3.Ras indicating active proliferative potential. Of note, p53 protein level was high in both F3 and F3.Ras cells that were derived by v-myc expression (Fig. 3d). Considering p53 protein stabilization by c-myc and p53 dependent stress respons, high protein level of p53 in both F3 and F3.Ras cells may result from expression of v-myc. However, in unidentified reason, F3 and F3.Ras lost p53 dependent transcriptional activity (Figs. 4, 5 and 6) and the molecular mechanism to govern the unexpected p53 response is currently under investigation.

F3.Ras Cells Develop Central Glial Tumor in Mice

We then attempted to determine whether F3.Ras cells could induce tumor formation under in vivo conditions. Six weeks after the intramuscular injection of F3 cells into the right thigh and F3.Ras cells into the left thigh of the experimental mice, the left thigh area (indicated by straight line, Fig. 4a) into which the F3.Ras cells had been injected developed tumors. Following the surgical extraction of the tumor mass, a clear difference was detected between the tumor masses originating from the F3 and F3.Ras cells (Fig. 4a, bottom panel). As is shown in Fig. 4b, tumor formation in the mice injected with F3.Ras was obvious. The gross appearance of the F3.Ras-induced tumor was that of a soft, polypoid tumor, composed of undifferentiated or poorly differentiated neuroepithelial cells. The microscopic appearance of the tumor is that of a cellular tumor composed of small uniform cells with scant fibrillar cytoplasm and oval configured nuclei with frequent mitotic populations. Tumor cells are arranged in lobules that harbor scattered rosettes (Fig. 4b). In order to further characterize the tumor tissue in detail, immunohistochemical studies have been carried out using antibodies including Ki-67, hNestin, and GFAP. A small portion of the entire tumor tissue tested positive for hNestin, thereby indicating that the neural stemness of injected F3.Ras cells may have been lost during cancer development. Cells positive for Ki-67, a proliferation antigen, were also relatively sparse, indicating that only a small number of F3.Ras cells retained proliferation potential subsequent to cancer development (Fig. 4c). These results are consistent with the immunohistochemical image, stained for the mitotic marker, phospho-H3. Only a few cells were positive for phospho-H3, which is consistent with the results of the Ki-67 immunohistochemistry (Fig. 4d). Unlike hNestin, which is expressed by only a small number of tumor cells, GFAP, which is widely employed as a cell-type specific

marker for glial differentiation, was more broadly positive (Fig. 4c and d). By way of contrast, tumor tissues from injections of U373 human glioma cells consisted of GFAP and Ki-67 positive populations with no clear Nestin-positive cells (Supplemental Figure 2). The results of fluorescent in situ hybridization (FISH) analysis with human probes demonstrated that the tumor tissue was derived from human cells into which the F3.Ras cells had been injected (Fig. 4e). These results demonstrate that F3.Ras cells form glial tumors consisting largely of GFAP-positive glial cells, in addition to a minor population of undifferentiated hNestin-positive neural stem cells.

F3.Ras Cells Develop Brain Tumors in the Mouse Brain

After intracerebral injection of F3.Ras cells, highly cellular tumor cells were located within the large portion of the cerebral hemisphere (Fig. 5a and b). These tumors were composed of undifferentiated or poorly-differentiated neuroepithelial cells. The tumor cells evidenced an ovoid morphology without prominent nuclei, and exhibited frequent mitoses. Geographic coagulative necrosis was also noted in these tumors. The tumor masses in the brains of the mice were immunostained with antibodies specific for human nuclear antigen (hNuA) in order to confirm that the tumor cells were of human origin. The tumor region was clearly distinguished by positive hNuA staining (Fig. 5c, bottom right panel). As in the cancer model from F3.Ras cells (Fig. 4c and d), hNestin and GFAP were expressed in the tumor tissues, but MAP2 was not—thus indicating that the F3.Ras cells had undergone an asymmetric self-renewal to either cancerous stem cells (Nestin positive) or astrocyte-like cells (GFAP positive), but not neurons (Fig. 5c and Supplemental figure 3). It is worth noting that hNestin-positive cells were more numerous in the brains into which F3.Ras cells were transplanted than in thigh muscle tissues similarly injected with F3.Ras cells (Fig. 4c).

Defective p53 Tumor-Suppressive Properties

Since normal primary human cells employ a variety of tumor-suppressive mechanisms and are resistant to oncogenic stresses such as H-Ras, the abrogation of tumor-suppressive mechanisms, particularly those involving p53, is regarded as a prerequisite for cellular transformation by H-Ras [10, 36]. In the case of F3.Ras cell generation, the parent v-myc-expressing hfNSC (F3) cells underwent oncogenic transformation via a single introduction of H-Ras in the absence of any further genetic modifications to abrogate p53; thus, it is conceivable that the F3 cells may possess a less active p53 tumor-suppressive mechanism. F3 and F3.Ras cells were subjected to a phospho-kinase profiler array in an effort to evaluate altered signaling as the result of the introduction of H-Ras. Taking into consideration the high levels of AKT phosphorylation (serine 473) and MEK1/2 phosphorylation (serine 218/222, serine 222/226) shown in the F3.Ras cells (iii, Fig. 6d), the profiler array was validated. A high level of p53 phosphorylation, which is indicative of the activation or increased stability of p53, was demonstrated in the F3.Ras cell lysates (i: serine 46, ii: serine 15). These results demonstrate that the introduction of H-Ras to F3 cells triggered p53 phosphorylation, which further activates p53-dependent tumor-suppressive mechanisms. To monitor the altered profile of p53-dependent genes after H-Ras introduction, the F3 cells were subjected to a p53 signaling pathway PCR array [37]. Among 13 genes that tested positive on the array, 11 genes—including *CDKN1A* and *NF1*—were reduced significantly relative to the F3 cells even after H-Ras introduction (Fig. 6b and

Supplemental table. 1). In particular, the tumor suppressor gene *NF1* encoding for neurofibromin 1 (Nf1), which is frequently suppressed or mutated in glioma or during gliomagenesis [38, 39] was detected at a significantly lower level after H-Ras introduction. These lowered Nf1 levels in F3.Ras cells were confirmed via immunoblotting analysis (Supplemental figure 4). Finally, we stimulated both F3 and F3.Ras cells with ultra-violet C (UVC) radiation and determined the Gadd45a mRNA levels, which corresponded closely with p53 transcriptional activity [40]. Similarly to the p53 null HCT116 cells, both F3 and F3.Ras cells failed to induce Gadd45α, whereas the p53 wild-type HCT116 cells induced Gadd45α mRNA after exposure to UVC radiation stress (Fig. 6c). The protein levels of p21 in the F3 and F3. Ras cells following treatment with nutlin3 (a chemical inhibitor of mdm2, which causes p53 accumulation) were significantly lower than those detected in the HCT116 wt cells (Fig. 6d). These results clearly indicate that F3 cells have defective p53 activity, which may be responsible for the oncogenic susceptibility of F3 cells observed after the introduction of H-Ras.

Susceptibility of F3 Cells to Oncogenic Stimulation

Lower p53-dependent transcriptional activity in F3 would be associated with tumorigenic potential as the result of a single oncogenic stimulation with H-Ras. To assess this, we transduced F3 cells with the oligodentrocyte lineage transcription factor Olig2 gene to generate oligodendrocytes (Fig. 7a). Oligodendrocytes derived from F3 cells (F3.Olig2) were negative for both hNestin, as shown by immunocytochemistry (Fig. 7a, left panel) and Sox2, as determined via RT-PCR (Fig. 7a, right panel); however, CNPase, an oligodendrocyte marker, was highly positive in the F3.Olig2 cells (Fig. 7a, bottom panel). In an effort to compare the oncogenic susceptibility, the colony formation of F3 cells was observed after the introduction of H-Ras. As demonstrated in Fig. 7b, the introduction of H-Ras to F3 cells induced the formation of colonies of cells with morphology typical of transformed cells, but this was not observed in the F3.Olig2 cells despite the stable expression of H-Ras and subsequent ERK activation similar to that of the F3 cells (Fig. 7b). In an effort to confirm the capability of H-Ras to transform either F3 or F3.Olig2 cells, identical numbers of cells after H-Ras introduction were seeded in soft agar. As anticipated, the introduction of H-Ras enabled colony formation by F3 cells but not by F3.Olig2 cells in the soft agar (Fig. 7c). These results demonstrate that F3.Olig2 cells, the differentiated counterparts of F3 cells, are not susceptible to H-Ras-mediated oncogenic stimulation, although this is not the case in F3 cells.

Discussion

Thus far, the oncogenic transformation of glial cells, which were previously thought to be the only proliferating cells in the brain, has generally been recognized as the origin of glioma or glioblastoma multiforme. The results of a previous study showed that human glioma cells were generated from human astrocytes via serial oncogenic stimulation with SV40 *T/t-Ag*, *hTERT*, and *H-ras^{v12G2}*. It has also been broadly accepted that the malignant transformation of human primary cells requires a complex oncogenic stimulation to overcome intrinsic tumor suppressive mechanisms, including the p53 and/or Rb tumor suppressors [41]. Therefore, the abrogation of p53 and/or Rb tumor-suppressive mechanisms

in human primary cells must first be achieved to induce malignant transformation, as in cases of introduction of SV40 T/t-Ag or E6/E7 [2, 42].

In this study, we demonstrated the successful transformation of human fetal NSCs via serial oncogenic stimulation only with v-myc and H-ras^{v12G} (Fig. 1). Considering the crucial functions of p53 in protecting cells against oncogenic transformation in a variety of cellular systems [43], the lower p53 transcriptional activity of v-myc-expressing hfNSCs (F3 cells), although its underlying mechanisms remain unknown (Fig. 6), may be responsible for the oncogenic transformation induced by a combination of v-myc and H-Ras. It is currently unclear as to the manner in which hfNSCs escape from apoptosis or cell cycle arrest when v-myc is introduced to effect cellular immortalization, as v-myc expression itself is sufficient to induce apoptosis or cellular senescence in a p53-dependent manner [44–46]. It is also worth noting that the oncogenic transformation induced by v-myc and H-Ras in hfNSCs did not occur when the hfNSCs lost neural stemness as the consequence of differentiation. After the differentiation of F3 cells into oligodendrocytes via the additional introduction of oligodendrocyte lineage transcription factor 2 (Olig2) as previously reported [47] and the consequent loss of neural stemness in those cells, the v-myc-expressing hfNSC cells were no longer susceptible to H-Ras-induced oncogenic transformations (Fig. 7). These findings indicate that the expression of an unknown factor or factors responsible for H-Ras-induced oncogenic transformation may vary according to the neural stemness characteristics. This may account for the differing susceptibility to oncogenic transformation between differentiated glial cells and NSCs [2]. In regard to cancer stem cells, which have been detected in various types of solid cancers, it remains unclear as to whether the F3.Ras cells generated in the present study are identical to the brain cancer stem cells isolated from a variety of gliomas, although we collected some evidence to suggest that F3.Ras cells share known common characteristics of brain cancer stem cells, such as sphere formation (Fig. 2d), ABCG2, ALDH1 expression, and EMT phenotypes (Fig. 3). However, the glial tumor formed by xenografted F3.Ras cells exhibited clear heterogeneity, consisting of a small portion of hNestin-positive and a larger portion of human GFAP-positive cells (Fig. 4). Considering that the tumor was composed of human-derived cells (Fig. 4e), these results show that a larger volume of GFAP-positive cells may be derived from a small number of Nestin-positive F3.Ras cells. Additionally, only a small number of cells were actively proliferating, as determined via staining with either Ki-67 proliferation antigen or phospho-Histone H3 antibody; this result differs from those seen with tumors generated from human glioma cell lines (Fig. 4c and d and Supplemental figure 2). These results are, however, consistent with the current cancer stem cell theory that a rare population of stem-like cancer cells can form heterogeneous cancers via asymmetric self-renewal, retaining rare populations of cancer stem cells. Thus, considering the shared properties of cancer stem cells, the F3.Ras cells should prove useful in further experiments, as a promising cellular platform for chemical drug-screening to find selective cancer stem cell inhibitors [48].

Interestingly, the p53 phosphorylation (serine 15 and serine 46) occurring in the N-terminal region of p53, which protects the p53 protein against degradation and enhances p53 transcriptional activity [49, 50], was detected following H-Ras introduction (Fig. 6a). Although the observed increase in p53 phosphorylation is suggestive of increased p53 transcriptional activity, p53-dependent transcription in F3 cells after H-Ras introduction was

shown to be suppressed relative to that observed in F3 cells (Fig. 6b, c and d). These results may indicate that different oncogenic susceptibility to H-Ras in F3 cells may result from defective p53 transcriptional activity and the consequent failure of tumor-suppressive mechanisms upon the introduction of H-Ras. We are currently attempting to assess which factor(s) (are) responsible for defective p53 transcriptional activity despite increases in phosphorylation. The alteration of acetylation status, another post-translational modification, the significance of which in the regulation of p53 transcriptional activity has been previously assessed [51], may be responsible for the repression of p53 transcriptional activity under high phosphorylation status conditions. This interesting research subject will also be assessed in greater detail in the future.

Collectively, the findings of this study demonstrate that hfNSCs underwent tumorigenic transformation via the introduction of the serial genes, v-myc and H-Ras, forming heterogeneous glial tumors with some characteristics of cancer stem cells. The tumors formed by F3.Ras cells were identified as heterogeneous glial tumors, and harbored small numbers of Nestin-positive neural stem-like cells. The F3.Ras cells are expected to prove applicable not only to inquiries into the molecular mechanisms relevant to cancer formation from the neural stem cells, but also as a valuable cellular platform for the screening of selective drugs for cancer stem cells.

Supplementary Material

Refer to Web version on PubMed Central for supplementary material.

Acknowledgments

References

1. Sanai N, Alvarez-Buylla A, Berger MS. Neural stem cells and the origin of gliomas. The New England Journal of Medicine. 2005; 353:811–822. [PubMed: 16120861]

2. Rich JN, Guo C, McLendon RE, Bigner DD, Wang XF, Counter CM. A genetically tractable model of human glioma formation. Cancer Research. 2001; 61:3556–3560. [PubMed: 11325817]

3. Zhu Y, Guignard F, Zhao D, et al. Early inactivation of p53 tumor suppressor gene cooperating with NF1 loss induces malignant astrocytoma. Cancer Cell. 2005; 8:119–130. [PubMed: 16098465]

4. Kwon CH, Zhao D, Chen J, et al. Pten haploinsufficiency accelerates formation of high-grade astrocytomas. Cancer Research. 2008; 68:3286–3294. [PubMed: 18451155]

5. Doetsch F, Caille I, Lim DA, Garcia-Verdugo JM, Alvarez-Buylla A. Subventricular zone astrocytes are neural stem cells in the adult mammalian brain. Cell. 1999; 97:703–716. [PubMed: 10380923]

6. Alvarez-Buylla A, Lim DA. For the long run: Maintaining germinal niches in the adult brain. Neuron. 2004; 41:683–686. [PubMed: 15003168]

7. Alcantara Llaguno SR, Chen J, Parada LF. Signaling in malignant astrocytomas: Role of neural stem cells and its therapeutic implications. Clinical Cancer Research. 2009; 15:7124–7129. [PubMed: 19934302]

8. Fan X, Eberhart CG. Medulloblastoma stem cells. Journal of Clinical Oncology. 2008; 26:2821–2827. [PubMed: 18539960]

9. Alcantara Llaguno S, Chen J, Kwon C, et al. Malignant astrocytomas originate from neural stem/progenitor cells in a somatic tumor suppressor mouse model. Cancer Cell. 2009; 15:45–56. [PubMed: 19111880]

10. Hahn WC, Counter CM, Lundberg AS, Beijersbergen RL, Brooks MW, Weinberg RA. Creation of human tumour cells with defined genetic elements. Nature. 1999; 400:464–468. [PubMed: 10440377]

11. Hahn WC. Immortalization and transformation of human cells. Molecules and Cells. 2002; 13:351–361. [PubMed: 12132573]

12. Rasheed BK, Wiltshire RN, Bigner SH, Bigner DD. Molecular pathogenesis of malignant gliomas. Current Opinion in Oncology. 1999; 11:162–167. [PubMed: 10328589]

13. Chen Z, Trotman LC, Shaffer D, et al. Crucial role of p53-dependent cellular senescence in suppression of Pten-deficient tumorigenesis. Nature. 2005; 436:725–730. [PubMed: 16079851]

14. Ferbeyre G, de Stanchina E, Lin AW, et al. Oncogenic ras and p53 cooperate to induce cellular senescence. Molecular and Cellular Biology. 2002; 22:3497–3508. [PubMed: 11971980]

15. Reilly KM, Loisel DA, Bronson RT, McLaughlin ME, Jacks T. Nf1;Trp53 mutant mice develop glioblastoma with evidence of strain-specific effects. Nature Genetics. 2000; 26:109–113. [PubMed: 10973261]

16. Flax JD, Aurora S, Yang C, et al. Engraftable human neural stem cells respond to developmental cues, replace neurons, and express foreign genes. Nature Biotechnology. 1998; 16:1033–1039.

17. Satoh JI, Obayashi S, Tabunoki H, Wakana T, Kim SU. Stable expression of Neurogenin 1 induces LGR5, a novel stem cell marker, in an immortalized human neural stem cell line HB1.F3. Cellular and Molecular Neurobiology. 2010; 30:415–426. [PubMed: 19813087]

18. Kim SU, Nagai A, Nakagawa E, et al. Production and characterization of immortal human neural stem cell line with multipotent differentiation property. Methods in Molecular Biology. 2008; 438:103–121. [PubMed: 18369753]

19. Arnold RS, Shi J, Murad E, et al. Hydrogen peroxide mediates the cell growth and transformation caused by the mitogenic oxidase Nox1. Proceedings of the National Academy of Sciences of the United States of America. 2001; 98:5550–5555. [PubMed: 11331784]

20. Kim SU, Park IH, Kim TH, et al. Brain transplantation of human neural stem cells transduced with tyrosine hydroxylase and GTP cyclohydrolase 1 provides functional improvement in animal models of Parkinson disease. Neuropathology. 2006; 26:129–140. [PubMed: 16708545]

21. Cai J, Wu Y, Mirua T, et al. Properties of a fetal multipotent neural stem cell (NEP cell). Developmental Biology. 2002; 251:221–240. [PubMed: 12435354]

22. Singh SK, Hawkins C, Clarke ID, et al. Identification of human brain tumour initiating cells. Nature. 2004; 432:396–401. [PubMed: 15549107]

23. Singh SK, Clarke ID, Terasaki M, et al. Identification of a cancer stem cell in human brain tumors. Cancer Research. 2003; 63:5821–5828. [PubMed: 14522905]

24. Hemmati HD, Nakano I, Lazareff JA, et al. Cancerous stem cells can arise from pediatric brain tumors. Proceedings of the National Academy of Sciences of the United States of America. 2003; 100:15178–15183. [PubMed: 14645703]

25. Bleau A, Hambardzumyan D, Ozawa T, et al. PTEN/PI3K/Akt pathway regulates the side population phenotype and ABCG2 activity in glioma tumor stem-like cells. Cell Stem Cell. 2009; 4:226–235. [PubMed: 19265662]

26. Patrawala L, Calhoun T, Schneider-Broussard R, Zhou J, Claypool K, Tang D. Side population is enriched in tumorigenic, stem-like cancer cells, whereas ABCG2+ and ABCG2- cancer cells are similarly tumorigenic. Cancer Research. 2005; 65:6207–6219. [PubMed: 16024622]

27. Ginestier C, Hur MH, Charafe-Jauffret E, et al. ALDH1 is a marker of normal and malignant human mammary stem cells and a predictor of poor clinical outcome. Cell Stem Cell. 2007; 1:555–567. [PubMed: 18371393]

28. Jiang T, Collins BJ, Jin N, et al. Achaete-scute complex homologue 1 regulates tumor-initiating capacity in human small cell lung cancer. Cancer Research. 2009; 69:845–854. [PubMed: 19176379]

29. Huang EH, Hynes MJ, Zhang T, et al. Aldehyde dehydrogenase 1 is a marker for normal and malignant human colonic stem cells (SC) and tracks SC overpopulation during colon tumorigenesis. Cancer Research. 2009; 69:3382–3389. [PubMed: 19336570]

30. Chen YC, Chen YW, Hsu HS, et al. Aldehyde dehydrogenase 1 is a putative marker for cancer stem cells in head and neck squamous cancer. Biochemical and Biophysical Research Communications. 2009; 385:307–313. [PubMed: 19450560]

31. Theodoropoulos PA, Polioudaki H, Agelaki S, et al. Circulating tumor cells with a putative stem cell phenotype in peripheral blood of patients with breast cancer. Cancer Letters. 2010; 288:99–106. [PubMed: 19619935]

32. Mani S, Guo W, Liao M, et al. The epithelial-mesenchymal transition generates cells with properties of stem cells. Cell. 2008; 133:704–715. [PubMed: 18485877]

33. Morel A, Lievre M, Thomas C, Hinkal G, Ansieau S, Puisieux A. Generation of breast cancer stem cells through epithelial-mesenchymal transition. PloS One. 2008; 3:e2888. [PubMed: 18682804]

34. Kabashima A, Higuchi H, Takaishi H, et al. Side population of pancreatic cancer cells predominates in TGF-beta-mediated epithelial to mesenchymal transition and invasion. International Journal of Cancer. 2009; 124:2771–2779.

35. DiMeo T, Anderson K, Phadke P, et al. A novel lung metastasis signature links Wnt signaling with cancer cell self-renewal and epithelial-mesenchymal transition in basal-like breast cancer. Cancer Research. 2009; 69:5364–5373. [PubMed: 19549913]

36. Mizumoto Y, Kyo S, Ohno S, et al. Creation of tumorigenic human endometrial epithelial cells with intact chromosomes by introducing defined genetic elements. Oncogene. 2006; 25:5673–5682. [PubMed: 16636665]

37. Brockschmidt C, Hirner H, Huber N, et al. Anti-apoptotic and growth-stimulatory functions of CK1 delta and epsilon in ductal adenocarcinoma of the pancreas are inhibited by IC261 in vitro and in vivo. Gut. 2008; 57:799–806. [PubMed: 18203806]

38. McGillicuddy LT, Fromm JA, Hollstein PE, et al. Proteasomal and genetic inactivation of the NF1 tumor suppressor in gliomagenesis. Cancer Cell. 2009; 16:44–54. [PubMed: 19573811]

39. Li Y, Bollag G, Clark R, et al. Somatic mutations in the neurofibromatosis 1 gene in human tumors. Cell. 1992; 69:275–281. [PubMed: 1568247]

40. Kastan M, Zhan Q, El-Deiry W, et al. A mammalian cell cycle checkpoint pathway utilizing p53 and GADD45 is defective in ataxia-telangiectasia. Cell. 1992; 71:587–597. [PubMed: 1423616]

41. Hahn WC, Weinberg RA. Rules for making human tumor cells. The New England Journal of Medicine. 2002; 347:1593–1603. [PubMed: 12432047]

42. Lundberg AS, Randell SH, Stewart SA, et al. Immortalization and transformation of primary human airway epithelial cells by gene transfer. Oncogene. 2002; 21:4577–4586. [PubMed: 12085236]

43. Eliyahu D, Michalovitz D, Eliyahu S, Pinhasi-Kimhi O, Oren M. Wild-type p53 can inhibit oncogene-mediated focus formation. Proceedings of the National Academy of Sciences of the United States of America. 1989; 86:8763–8767. [PubMed: 2530586]

44. Kim HS, Shin JY, Yun JY, Ahn DK, Le JY. Immortalization of human embryonic fibroblasts by overexpression of c-myc and simian virus 40 large T antigen. Experimental & Molecular Medicine. 2001; 33:293–298. [PubMed: 11795494]

45. Hermeking H, Eick D. Mediation of c-Myc-induced apoptosis by p53. Science. 1994; 265:2091–2093. [PubMed: 8091232]

46. Yu K, Ravera C, Chen Y, McMahon G. Regulation of Myc-dependent apoptosis by p53, c-Jun N-terminal kinases/stress-activated protein kinases, and Mdm-2. Cell Growth & Differentiation. 1997; 8:731–742. [PubMed: 9218867]

47. Ahn SM, Byun K, Kim D, et al. Olig2-induced neural stem cell differentiation involves downregulation of Wnt signaling and induction of Dickkopf-1 expression. PloS One. 2008; 3:e3917. [PubMed: 19093005]

48. Gupta PB, Onder TT, Jiang G, et al. Identification of selective inhibitors of cancer stem cells by high-throughput screening. Cell. 2009; 138:645–659. [PubMed: 19682730]

49. Shieh SY, Ikeda M, Taya Y, Prives C. DNA damage-induced phosphorylation of p53 alleviates inhibition by MDM2. Cell. 1997; 91:325–334. [PubMed: 9363941]

50. D'Orazi G, Cecchinelli B, Bruno T, et al. Homeodomain-interacting protein kinase-2 phosphorylates p53 at Ser 46 and mediates apoptosis. Nature Cell Biology. 2002; 4:11–19.

51. Tang Y, Zhao W, Chen Y, Zhao Y, Gu W. Acetylation is indispensable for p53 activation. Cell. 2008; 133:612–626. [PubMed: 18485870]
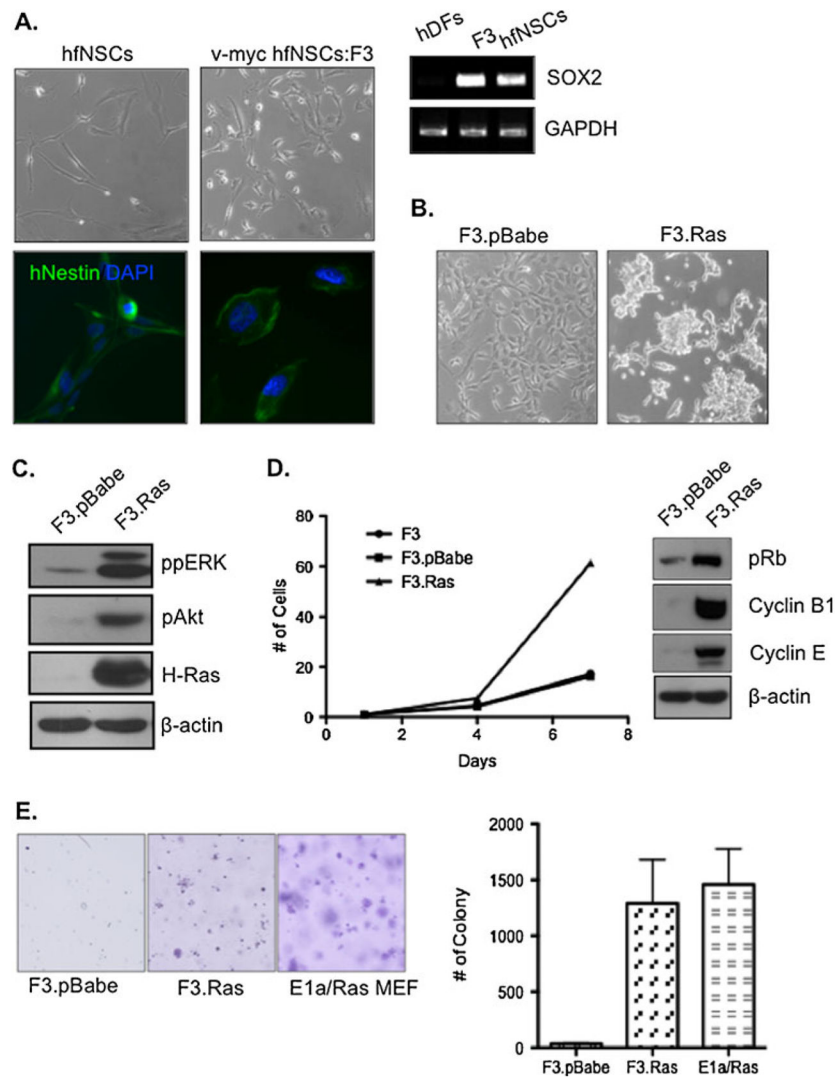
Fig. 1.

v-myc and H-Ras introduction was sufficient for oncogenic transformation of hfNSCs. **a** Morphology of hfNSCs and v-myc-expressing hfNSCs (F3 cells) were presented as light microscopic images (upper panels). The neural stem cell marker, hNestin (*green*), is expressed in both ftNSCs and F3 cells. DAPI (*blue*) was used for nuclear counter-staining. Another neural stem cell marker, Sox2, was detected via RT-PCR analysis. GAPDH was used for equal loading control. **b** Morphological changes of F3. pBabe and F3.Ras were depicted as light microscopic images. **c** Mitogenic signals such as phospho-ERK and phospho-Akt in F3 immortalized neural stem cells with empty vector (F3. pBabe) were compared to H-Ras-expressing F3 cells (F3. Ras) via immunoblotting analysis. β-actin was employed as a loading control. **d** Accelerated proliferation in F3.Ras relative to F3.pBabe and F3 cells was determined by cell counting on each of the indicated days and presented as a graph (left panel). Higher levels of a variety of cell cycle regulators in F3.Ras cells such as cyclin B1, cyclin E, and phospho-Rb were determined via immunoblotting analysis (right panel). **e** Levels of colony formation of each indicated cell in soft agar (left panel) were

determined by the number of colonies, and then graphically presented (right panel). E1a/Ras MEF was used as a positive control
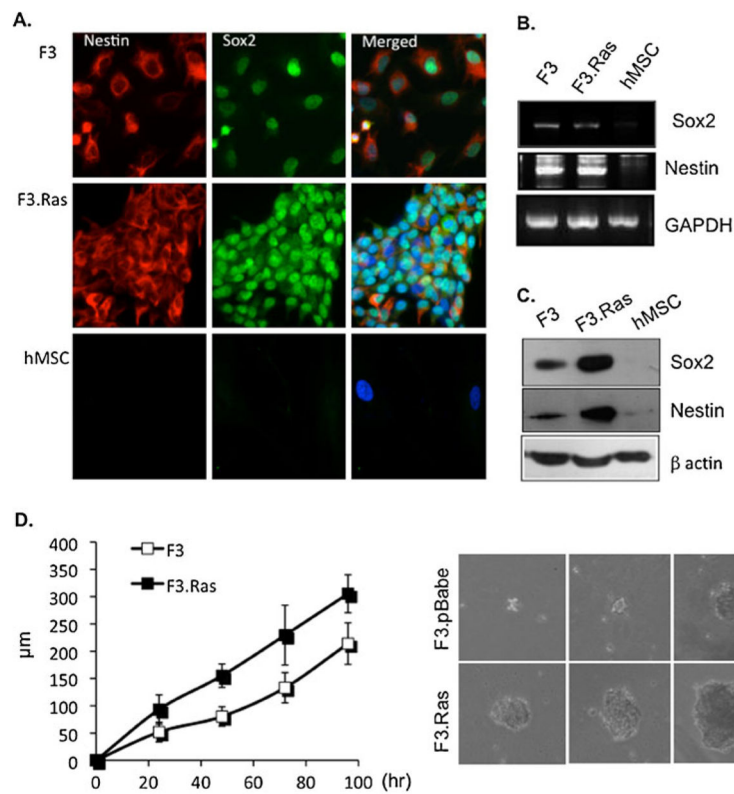
Fig. 2.
F3.Ras cells retain neural stemness. **a** The neural stem cell markers, hNestin (*red*) and Sox2 (*green*) are co-expressed in F3 and F3.Ras cells. Human mesenchymal stem cells (hMSCs) were employed as negative controls for Nestin and Sox2 staining. **b** RT-PCR analysis of Sox2 and Nestin levels in F3 and F3.Ras cells. GAPDH was used as a DNA loading control. **c** Sox2 and Nestin levels in F3 and F3.Ras cells were determined via immunoblotting analysis. β-actin was employed as a protein loading control. **d** Neurosphere formation between F3.pBabe and F3.Ras was compared on various days (right panel). Diameters of more than 12 spheres of F3.pBabe and F3.Ras were measured and the average values were graphically presented
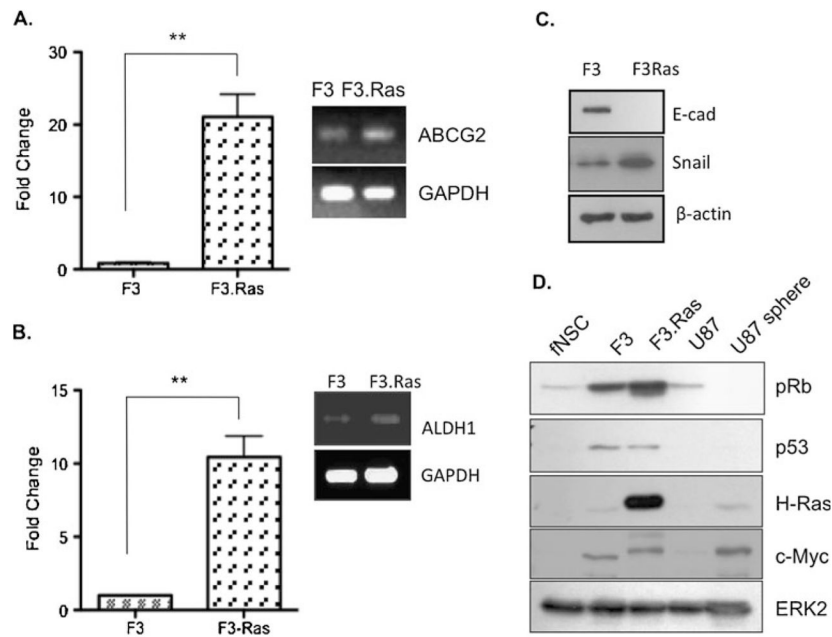
Fig. 3.
F3.Ras cells may share characteristics of neural cancer stem cells. **a** mRNA levels of
ABCG2 were determined via real-time PCR (left panel) and RT-PCR (right panel). (**, *p*
<0.05). **b** The mRNA level of ALDH1 was determined via real-time PCR (left panel) and
RT-PCR (right panel). (**, *p* <0.05). **c** The levels of E-cadherin and Snail in F3 and F3.Ras
cells were determined via immunoblotting. β-actin was used as a loading control. **d** The
level of c-myc, Ras, pRB and p53 for the hfNSC, F3, F3.Ras, U87 and U87 sphere were
determined by immunoblotting analysis. ERK2 was used as a loading control
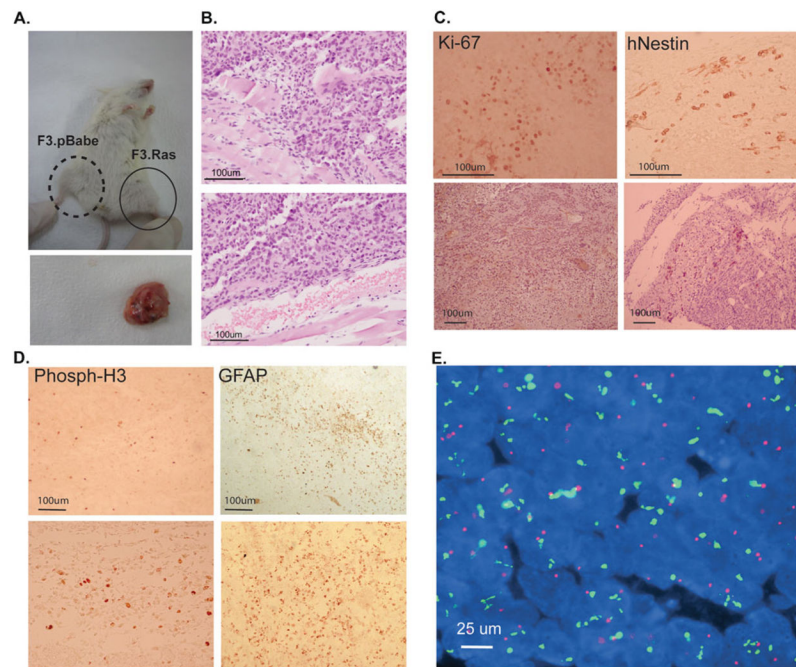
Fig. 4.
F3.Ras cells form tumors in mice. **a** NOD/SCID male mice at 6 weeks of age were injected intramuscularly with 1×10^6 of F3.pBabe (left thigh: *dotted line*) or F3.Ras cells (right thigh: *solid line*), and tumor appearance after 6 weeks was assessed. Tumor masses from the right thigh area injected with F3.Ras cells were isolated and processed for histologic analysis (right panel). **b** Tissues isolated from the tumor mass were stained with hematoxylin and eosin (H/E), and the tumors were identified. **c** Tumor tissues were immunostained with proliferation markers (phospho-Histone H3) and cell type-specific marker for astrocytes (GFAP). Bar indicates 100 μm. **d** Tumor tissues were immunostained with proliferation marker (Ki-67) and cell type-specific marker for neural stem cells (hNestin:). Lower panels are H/E staining images. **e** FISH with human chromosome probe on mouse tumor tissue (LSI21 for *red*, CEP18 for *green*). DAPI for nuclear counterstaining
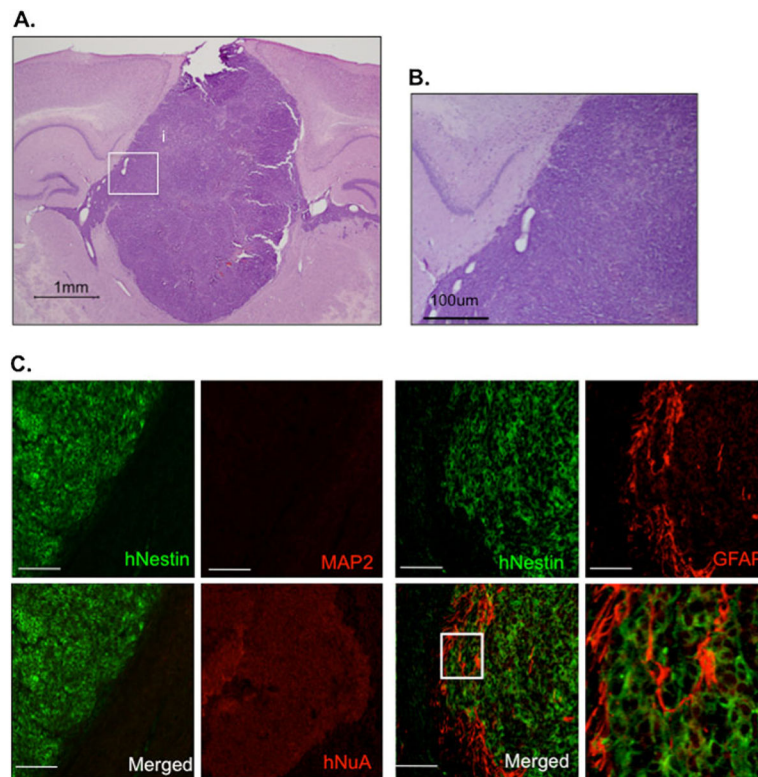
Fig. 5.
F3.Ras cells form brain tumor in mice. **a** Brain tumor formed following the intracerebral injection of F3.Ras cells. **b** H/E staining of indicative areas (i and ii) at higher magnification. (C) hNestin, GFAP and MAP2 were immunostained. Human nuclei (hNuA) staining conducted to show human cell-derived cancer area. Bar:100 μm. *White box* (right bottom panel) was enlarged at higher magnification
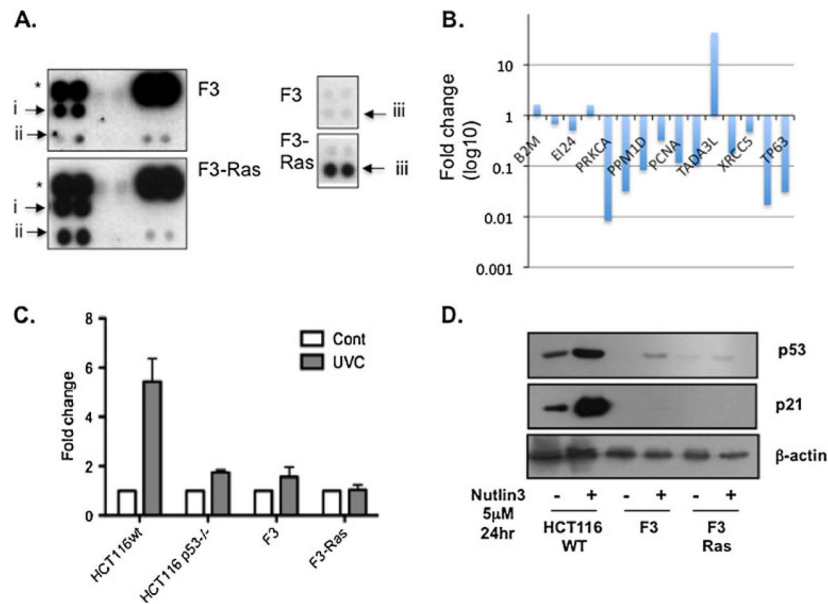
Fig. 6.
Defective p53 response in F3 cells (**a**) Multiple signaling changes in F3.Ras were assessed using a phospho-kinase profiler array kit. Levels of p53 phosphorylation on serine 46 (i) and serine 15 (ii) and AKT phosphorylation on serine 473 (iii) on either F3 (upper panel) and F3.Ras (lower panel) are displayed. * for positive control for equal loading of sample. (**b**) Fold change of mRNA level of 13 p53-dependent genes of F3.Ras compared to F3.pBabe was presented graphically (Y axis: log 10, bottom panel). (**c**) Gadd45a mRNA level after 10 J/m^2 of UVC on each of the indicated cells were determined via real-time PCR analysis and graphically presented. Means and SEM were determined from three independent studies. (**d**) p53 and p21 protein levels after 24 h of nutlin3 treatment were determined via immunoblotting analysis. β-actin was used for loading control
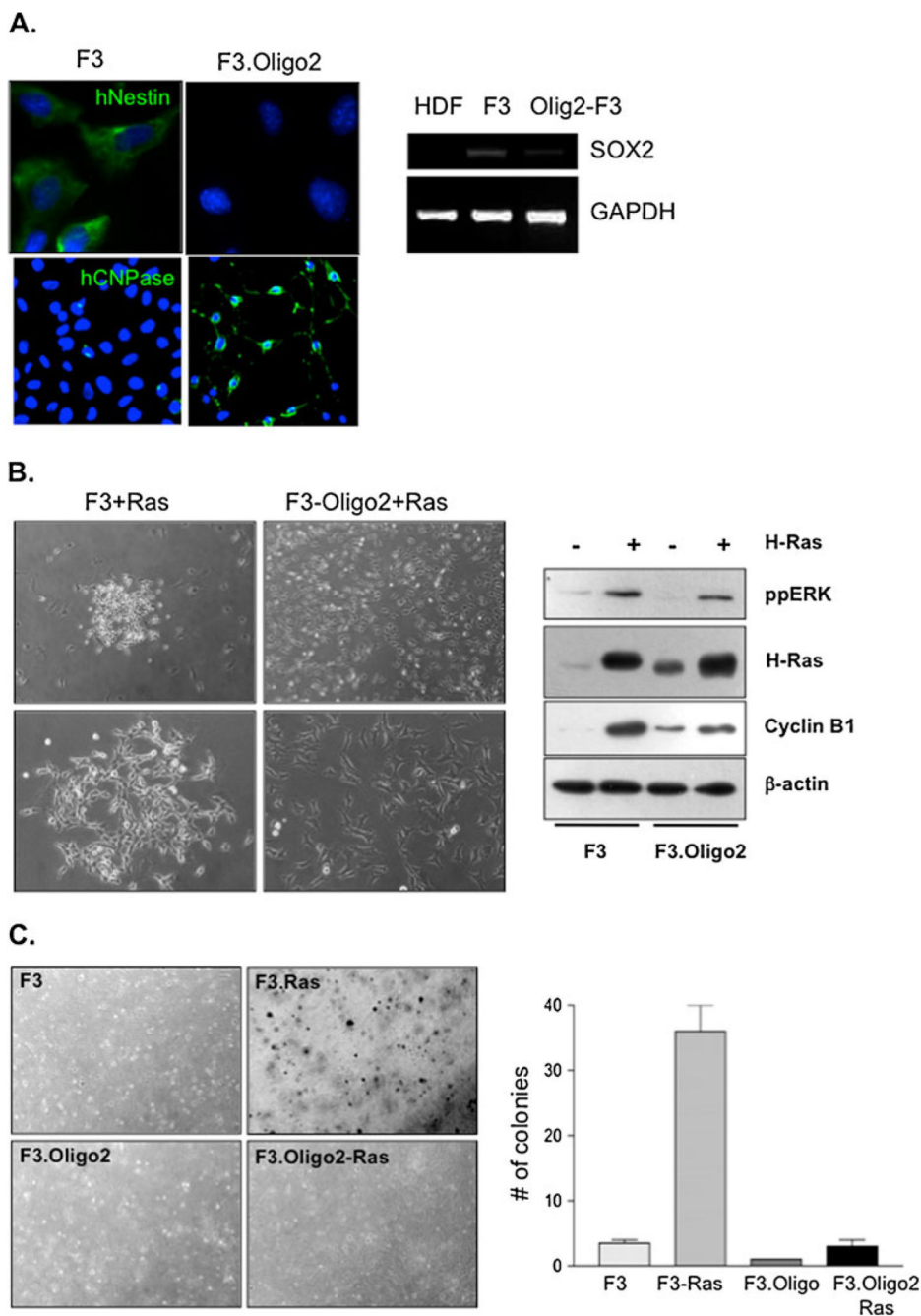
A.

B.

C.

Fig. 7.
Different oncogenic susceptibility of F3 compared to F3.Olig2 (**a**) F3 and F3.Olig2 cells were immunostained with hNestin (*green*, top panels), human CNPase (*green*, bottom panels) and counterstained with DAPI (*blue*). Merged images were shown (left panel). Sox2 level from human dermal fibroblasts (hDFs), F3 and F3.Olig2 was determined via RT-PCR analysis. GAPDH was used for equal loading (right panel). (**b**) Morphological change of F3 and F3.Olig2 after H-Ras introduction was presented (top panel: 100X, bottom pane: 200X). phospho ERK, H-Ras and cyclin B1 level were determined via immunoblotting analysis. β-

actin was used for loading control. (**c**) The level of colony formation in the soft-agar of each of the indicated cells (left panel) was determined by the number of colonies, and then graphically presented (right panel)